Effect of infiltration characteristics of soil on tree stability

A. Rahimi, H. Rahardjo, E.C. Leong, T.T. Lee, A.W.K. Law
Nanyang Technological University, Singapore

Y.K. Fong
National Parks Boards, Singapore

ABSTRACT: Tree failures occur frequently in Singapore. Tree failures are often catastrophic to public and infrastructure of a densely populated urban environment like Singapore. Soil properties, rainfall condition, wind condition and green wood properties are main factors that contribute to tree stability. In this paper, the effect of infiltration characteristics of soil on tree stability is investigated through numerical modelling. A typical residual soil of Singapore was subjected to different rainfall conditions to study its infiltration characteristics and its effect on tree stability. The results of the analyses show that hydraulic properties of the soil have significant effects on infiltration characteristics of the soil and consequently on tree stability.

1 INTRODUCTION

Tree failures during rain storm have been reported worldwide, including Singapore. The tropical climatic condition of Singapore results in abundance of rainfall. In 2010, NParks reported approximately 1400 cases of tree failure in Singapore (NParks, 2011). These events have caused economic losses and even serious injuries and deaths. (Straits Times, April 2013). Therefore, it is important to identify the cause of tree failures and ways to prevent them. The soil used for tree planting is usually well above the ground water table and is usually in an unsaturated condition. The shear strength of the unsaturated soil is governed by two independent stress-state variables, matric suction (negative pore-water pressure) and net normal stress (Fredlund and Rahardjo, 1993). Infiltration of rainwater into the soil reduces the negative pore-water pressure which in turn reduces the shear strength of the soil. This would result in a reduction in resistance of the tree against uprooting. Infiltration of rainwater into the soil depends on the hydraulic properties of the soil. Limited studies have been conducted to investigate the relationship between rainfall and tree failure. Koizumi (1987) conducted several tree-pulling experiments and showed that stability of a tree after rainfall is lower than stability of a similar tree in soil without occurrence of rainfall. However, limited studies investigated the effect of infiltration characteristic of soil on tree stability. Therefore, it is essential to understand the stability of trees planted in different soils with different infiltration characteristics.

2 METHODOLOGY

In order to investigate the effect of infiltration characteristics of soil on tree stability, two different soil types were selected to represent good drainage (GD) and poor drainage (PD) residual soils of Singapore. The GD and PD soils were subjected to a rainfall of 1×10^{-6} m/s for a duration of 24 hours. Seepage analysis was performed to compute the pore-water pressure changes due to the rainfall. The computed pore-water pressures were then used as initial condition to conduct load/deformation analysis in order to assess the stability of a tree subjected to wind load. A wind load of 150 kN was used in the load/deformation analyses. The pore-water pressures at initial time before the rainfall; at time equal to 12 hours and at time equal to 24 hours (i.e., end of the rainfall) were imported in load/deformation analyses as initial pore-water pressures. The induced strain in the root plate and soil was observed and compared at different times during the rainfall. Tree instability or failure was assumed to have occurred when the soil experienced more than 15% strain (ASTM D4767-11, 2011) or the tree or root plate experienced more than 5% strain at its extreme fibers (Lee, 2015).

3 NUMERICAL MODELING

Seepage analyses were conducted using a numerical model of simplified tree-root-soil model using SEEP/W (Geo-slope International, 2012a) software. A tree of 10 m height and 0.5 m width with a root plate of 0.25 m thickness and diameter of 5.5 m surrounded by a soil block of 20 m width and 10 m height was considered for the analyses as shown in Figure 1. The dimensions of tree and root plate were selected based on the recommendation by NParks (2009). The infiltration process of the rainwater into the soil was conducted using a saturated-unsaturated, finite element seepage analysis. The boundary conditions applied to the tree-root-soil model are also shown in Figure 1. A boundary flux, q, equal to rainfall intensity, Ir = 10-6 m/s was applied to the surface of the model. The nodal flux, Q, equal to zero was applied along the sides of the soil to simulate no flow zone. The water table was assumed to be at the bottom of the model (i.e., 10 m depth). A boundary flux, ET, equal to evapotranspiration was applied to the root plate boundaries.

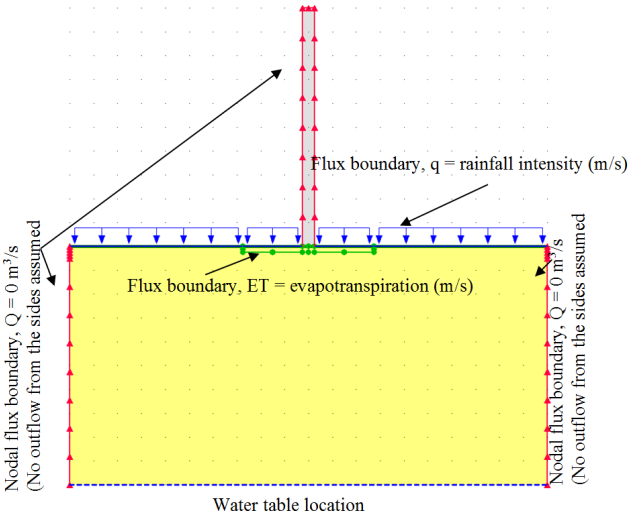

Figure 1. Finite element model and initial condition for the tree-root-soil model

Soil-water characteristic curve (SWCC) and permeability functions are two primary soil properties used in the seepage analysis as shown in Figure 2 for both of GD and PD soils.

The saturated coefficient of permeability of GD soil, k_s, was equal to 10^{-4} m/s and SWCC parameters of the soil were a=10 kPa, m=0.5 and n=1. The saturated coefficient of permeability of PD soil was equal to 10^{-6} m/s. SWCC parameters of PD soil were a=300 kPa, m=1 and n=1. The detailed explanation of the two selected soils can be found in Rahimi et al. (2010).

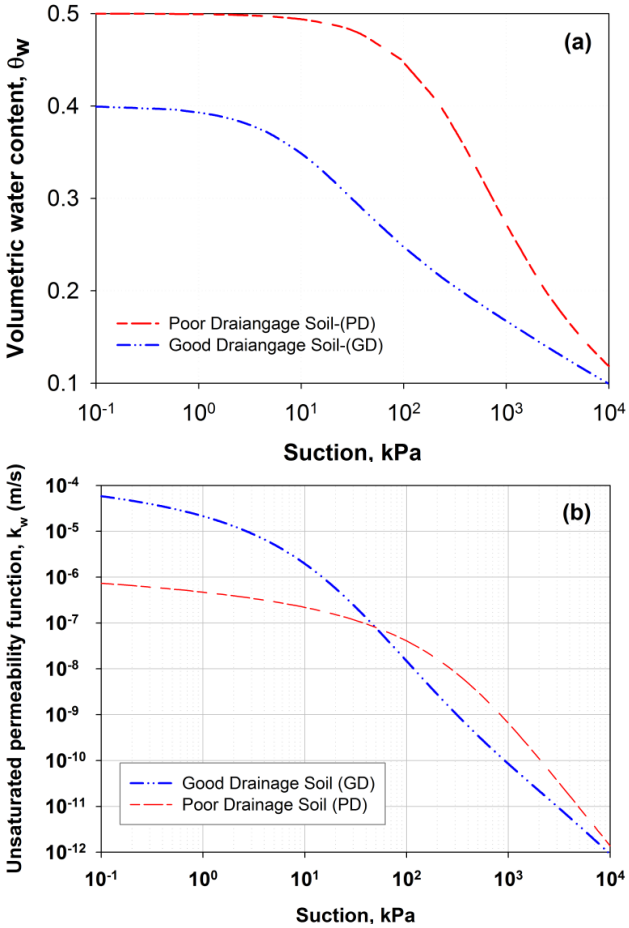

Figure 2. Soil hydraulic properties of GD and PD soils used in numerical modelling: (a) soil-water characteristic curve, (b) unsaturated permeability function

The water-flow governing equation used in the software for solving a transient and two dimensional seepage analysis is as follows:

$$m_w^2 \gamma_w \frac{\partial h_w}{\partial t} = \frac{\partial}{\partial x}\left(-k_{wx}\frac{\partial h_w}{\partial x}\right) + \frac{\partial}{\partial y}\left(-k_{wy}\frac{\partial h_w}{\partial y}\right) + q \qquad (1)$$

where m_w^2=slope of soil-water characteristic curve; γ_w= unit weight of water; h_w= hydraulic head or total head; t = time; k_{wx}= coefficient of permeability with respect to water as a function of matric suction in x-direction; k_{wy}= coefficient of permeability with respect to water as a function of matric suction in y-direction; and q = applied flux at the boundary. The pore-water pressures was computed by seepage analyses and used as initial pore-water pressures for load/deformation analyses. SIGMA/W (Geo-slope International, 2012b) software was used for the load/deformation modelling of the tree stability. The model was a two-dimensional plane strain model. The mesh of the root and the surrounding soil consists of rectangular elements. Friction between soil and root was ignored. The boundary conditions of the tree-root-soil model are shown in Figure 3. Horizontal displacement was fixed on both vertical boundaries, and displacements in both directions were fixed on the bottom boundary of the model as shown in Figure 3.

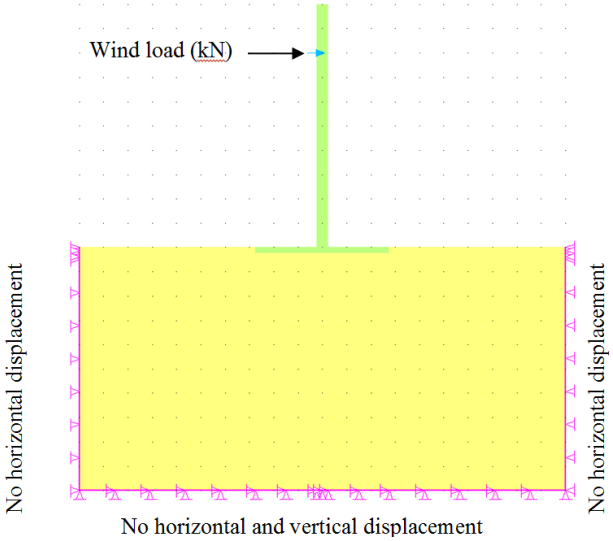

Figure 3-Boundary condition and schematic diagram of tree-root-soil model used in load/deformation analyses

For load/deformation analyses, the soil was modelled as an elastic–plastic material. The elastic part was governed by modulus of elasticity, E, and Poisson's ratio, μ, of the soil. Typical values of 10000 kPa and 0.4 were assumed for the modulus of elasticity and Poisson's ratio of the soil, respectively. Root-plate material was considered as a linear-elastic material with a modulus of elasticity of 1200000 kPa and a Poisson's ratio of 0.3 (Lee, 2015). Typical shear strength properties of Singapore residual soils (Rahardjo et al., 2007) were selected for both GD and PD soils. An effective cohesion, c′=10 kPa, effective angle of internal friction, ϕ'=26 degrees, and unit weight of soil, γ=20 kN/m^3 were used in the analyses. Table 1 shows the soil properties and Table 2 shows the root plate and tree properties used in the study.

Table 1. Soil properties.

	E modulus (kPa)	Unit weight (kN/m^3)	Poisson's ratio	Friction angle (°)	Cohesion (kPa)
Soil	10000	20	0.4	26	10

Table 2. Root plate and tree properties

	E modulus (kPa)	Unit weight (kN/m^3)	Poisson's ratio	Height (m)	Trunk Diameter (m)	Root Plate Tickness (m)	Root Plate Diameter (m)
Root plate and Tree	1200000	10	0.3	10	0.5	0.25	5.5

4 RESULTS AND DISSCUSSION

The results of seepage analyses for t = 0, t = 12 h and t = 24 h were used as initial pore-water pressures in load/deformation analyses. The induced strains in the tree, root and soil due to the applied wind load on the tree were observed and presented below.

The strain profiles are shown at three locations, namely trunk base, root plate base and soil as shown in Figure 4.

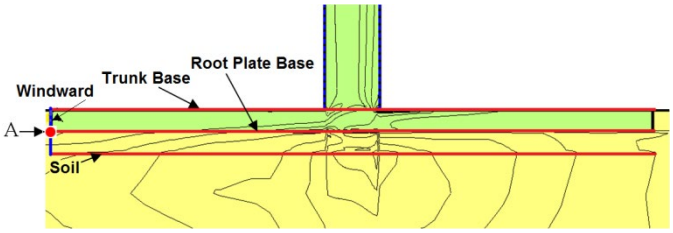

Figure 4. Location of the observed strains in the trunk base, root plate base and soil

The resulting strains at the trunk base for GD and PD soils are shown in Figure 5 at different times during the rainfall. As shown in the figure, the windward side of the trunk base experienced tension and the leeward side of the trunk base experienced compression as reflected by the positive and negative values of strains, respectively for both of GD and PD soils. The maximum magnitude of the tension strain and compression strain at the trunk base was 2.3 % (t = 0 h) and -3.2 % (at t = 24 h), respectively, for both of GD and PD soils. The tree and root plate properties were the same for both of PD and GD soils. In addition the pore-water pressure changes due to the applied rainfall did not affect the tree and root plate properties. As a result, the strains at the trunk base were more or less the same during the rainfall and they were similar in both soils. The change in the strain due to the applied rainfall was negligible and it remained under 5 % at all times. Therefore, it can be concluded that the tree trunk did not experience any failure at all times.

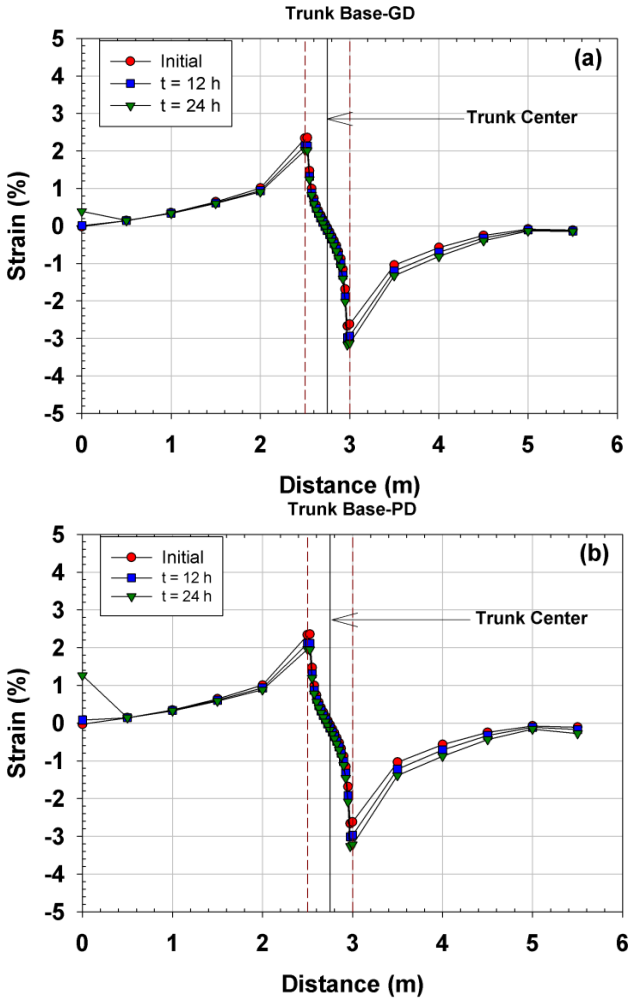

Figure 5. Strains profile in the trunk base: (a) GD soil, (b) PD soil.

The resulting strains at the root plate base for GD and PD soils are shown in Figure 6 at different times during the rainfall. As shown in the figure, the windward side of the root plate base experienced tension and the leeward side of the root plate base experienced compression as reflected by the positive and negative values of strains, respectively, for both of GD and PD soils. As shown in the figure, the tension strain increased significantly due to the applied rainfall, while the compression strain increased marginally for both of GD and PD soils. The maximum magnitude of the compression strain at the root plate base was -2.1 % (t = 24 h) for GD soil and -2.1 % (t = 12 h) for PD soil which remained under 5 % at all times. However, the tension strains increased from 2.5 % (t = 0 h) to 4.7 % (t = 24 h) near the trunk and from 0.8 % (t = 0 h) to 10.8 % (t = 12 h) and 14 % (t = 24 h) at the edge of the root plate for GD soil. On the other hand, the tension strains increased from 2.5 % (t = 0 h) to 5.6 % (t = 24 h) near the trunk and from 0.8 % (t = 0 h) to 12 % (t = 12 h) and 17 % (t = 24 h) at the edge of the root plate for PD soil. The significant increase in tension strain at the base of the root plate (i.e., larger than 5 %) reflected the failure of the tension roots due to the presence of rainfall. It can be seen that the increase in strains in root plate base due to the rainfall was larger in PD soil as compared to that in GD soil. This was due to the higher permeability of GD soil which resulted in a faster infiltration of rainwater into the soil. As a result, the increase in pore-water pressures in GD soil was less as compared to that of PD soil. For instance, the pore-water pressure at point A (see Figure 4) increased from -94.6 kPa (t = 0 h) to -48 kPa (t = 12 h) and -30 kPa (t = 24 h) in GD soil whereas it increased from -93 kPa (t = 0 h) to -38 kPa (t = 0 h) and -11 kPa (t = 0 h) in PD soil. As a result, the decrease in the shear strength of the soil was less in GD soil as compared to that of PD soil. Therefore, the induced tension strains in GD soil were smaller than that of PD soil.

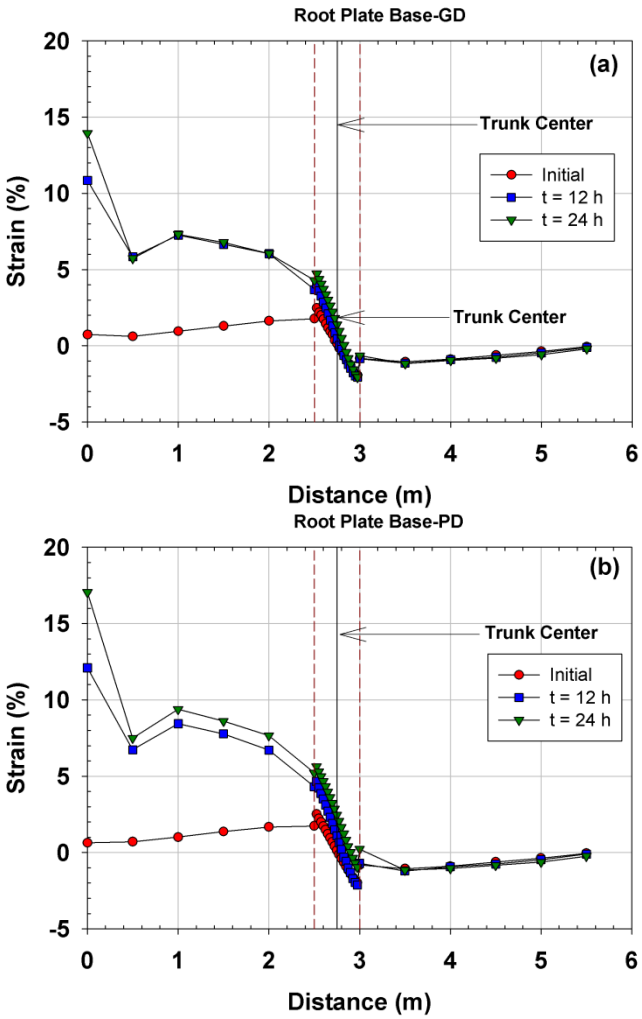

Figure 6. Strains profile in the root plate base: (a) GD soil, (b) PD soil

The resulting strains at the soil (see Figure 4) for GD and PD soils are shown in Figure 7 at different times during the rainfall. As shown in the figure, the windward side of the soil experienced tension and the leeward side of the soil experienced compression as reflected by the positive and negative values of strains, respectively, for both of GD and PD soils. As shown in the figure, the tension strain increased significantly due to the applied rainfall, while the compression strain increased slightly. The magnitude of tension strains in the soil increased as the

distance from the trunk increased significantly due to the presence of rainfall. For instance, the tension strain in the soil underneath the edge of the root plate increased from 0.8 % (t = 0 h) to 11.1 % (t = 12 h) and 17.4 % (t = 24 h) in GD soil. On the other hand, the tension strain in the soil underneath the edge of the root plate increased from 0.7 % (t = 0 h) to 12.7 % (t = 12 h) and 22.5 % (t = 24 h) in PD soil. The significant increase in the tension strains reflected the failure of the soil at windward side. Therefore, if any root existed at that location it may experience tension failure as well which potentially could cause the failure of the tree due to root break.

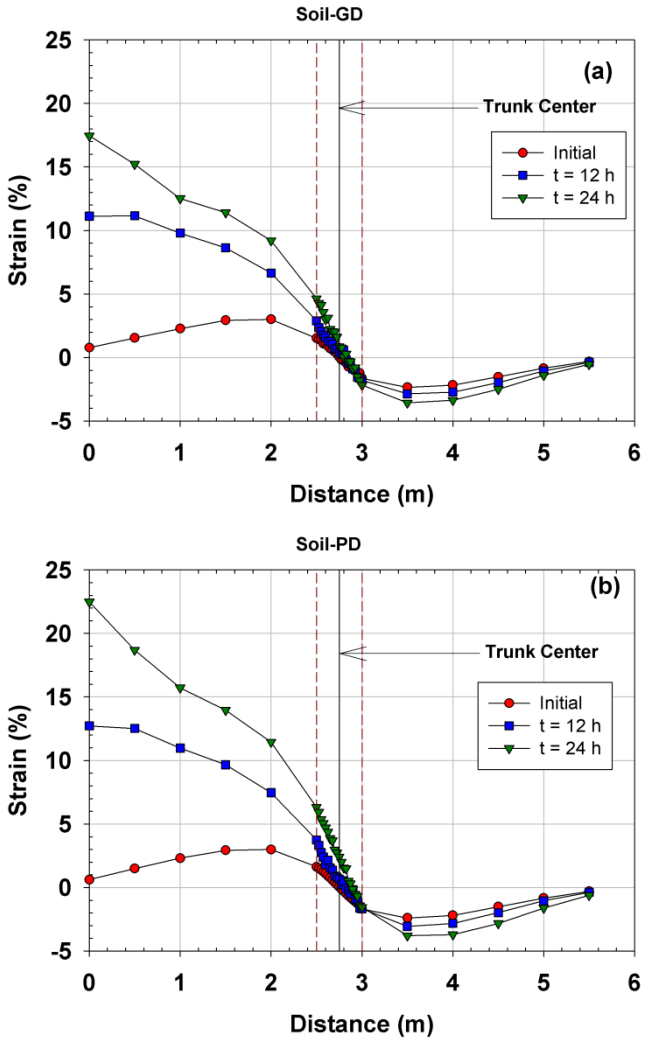

Figure 7. Strains profile in the soil: (a) GD soil, (b) PD soil

5 CONCLUSIONS

Based on the seepage and load/deformation analyses of the tree-root-soil model subjected to rainfall of 1×10^{-6} m/s and wind load of 150 kN, it was found that the presence of rainfall significantly increased the tension strains which resulted in tree failure. The lower permeability of PD soil resulted in a slower infiltration of rainwater into the soil. As a result, the increase in pore-water pressures in PD soil was larger as compared to that of GD soil. Therefore, the increase in tension strain was higher in PD soil as compared to GD soil.

6 ACKNOWLEDGEMENT

The study was carried out as a part of a research collaboration to study effect of rainfall on tree stability. The study was conducted by the Nanyang Technological University and National Parks Board, Singapore with some financial supports from DHI-NTU.

REFEREENCES

ASTM D4767-11. 2011. Standard Test Method for Consolidated Undrained Triaxial Compression Test for Cohesive Soils.

Fredlund, D. G. and Rahardjo, H., 1993. Soil mechanics for unsaturated soils. Wiley, New York.

Geo-slope International, 2012. SEEP/W for finite element seepage analysis, user's guide. Calgary, Alta., Canada.

Koizumi, A., Motoyama, J., Sawata, K., Sasaki, Y., & Hirai, T., 2010. Evaluation of drag coefficients of poplar-tree crowns by a field test method. The Japan Wood Research Society, 56: 189-193.

Lee, T. T., 2015. Effect of rainfall on tree stability. PhD Thesis under examination. Nanyang Technological University, Singapore

National Parks Board., 2011. Conservation of Trees /Plants.

Rahardjo, H., Ong, T.H., Rezaur, R.B. and Leong E.C., 2007. Factors controlling instability of homogeneous soil slopes under rainfall. Journal of Geotechnical and Geoenvironmental Engineering, ASCE, 133(12): 1532-1543.

Rahimi, A., Rahardjo, H., and Leong, E.C. 2010. Effect of antecedent rainfall patterns on rainfall-induced slope failure. Journal of Geotechnical and Geoenvironmental Engineering, 137(5): 483-491.